ELSEVIER

Thermochimica Acta 346 (2000) 91–103

thermochimica acta

www.elsevier.com/locate/tca

Kinetic and thermodynamic study of the non-isothermal decompositions of cobalt malonate dihydrate and of cobalt hydrogen malonate dihydrate

Mohamed A. Mohamed[a,*], Andrew K. Galwey[b], Samih A. Halawy[c]

[a]*Chemistry Department, Faculty of Science, South Valley University, Qena 83523, Egypt*
[b]*School of Pharmacy, Queen's University of Belfast, Belfast BT9 5AG, Ireland*
[c]*Chemistry Department, College of Education, King Faisal University, PO Box 1759, Al-Hofouf 31982, Eastern Province, Saudi Arabia*

Received 8 July 1999; received in revised form 5 October 1999; accepted 6 October 1999

Abstract

Non-isothermal dehydrations and decompositions of cobalt malonate dihydrate and of cobalt hydrogen malonate dihydrate were studied between ambient temperature and 500°C. Different thermal analyses techniques (including TG, DTG, DTA and DSC) were used. The thermal reactions of both salts were performed in different dynamic atmospheres (40 ml/min) of N_2, H_2 or air. Cobalt hydrogen malonate was found to decompose at an appreciably lower temperature compared with cobalt malonate. Kinetic and thermodynamic parameters for the reactions of both reactant salts were calculated.

IR spectroscopy of the partially decomposed samples showed that cobalt acetate and cobalt carbonate were formed as reaction intermediates during the breakdowns of both salts. This formation of cobalt acetate, a probable participant in the reaction, took place at an appreciably lower temperature for the cobalt hydrogen malonate reactant.

X-ray diffraction revealed that the solid decomposition products were identical from both cobalt malonate and cobalt hydrogen malonate, under the same dynamic atmosphere. Cobalt metal was the major solid product in H_2 and N_2, while Co_3O_4 was the product in an atmosphere of air. Gas chromatography was used to identify the volatile decomposition products which included CO_2, CO, acetic acid, acetone and traces of esters.

It is concluded that, following dehydration, cobalt hydrogen malonate decomposes to cobalt malonate, and subsequent reactions were closely similar to those for this prepared reactant. Decomposition of cobalt malonate is identified as being controlled by an electron transfer step and proceeding at the active surface of the solid product. Cobalt metal is formed by reaction in hydrogen and cobalt oxide, Co_3O_4, in air. The slightly higher temperatures required for reaction in nitrogen are ascribed to deactivation of the product surface by deposited carbonaceous residues.

Keywords: Decomposition; Cobalt malonate dihydrate; Cobalt hydrogen malonate hydrate; TG; DTA; DSC; XRD; IR; GC; Kinetics

1. Introduction

There have been extensive studies of the thermal decompositions of metal carboxylates. The courses of

* Corresponding author. Tel.: +20-96-211273; fax: +20-96-211272.
E-mail address: sci@svalleyu.jwnet.eun.eg (M.A. Mohamed).

0040-6031/00/$ – see front matter
PII: S0040-6031(99)00376-7

these reactions have been shown to be influenced by both the constituent cation and the anion of the salt, as well as reaction conditions, including the prevailing atmosphere [1–6]. Comparative investigations have often been directed towards determining the changes in reactivity and of stoichiometry that occur for reactants that form a series containing a common constituent, either anion or cation. Reactants selected as being of interest have usually included the simplest carboxylates and many such studies have been concerned with the metal malonates.

The Group IIA metal malonates, including the Be, Mg, Ca, Sr and Ba salts, decomposed [7] without change in the valence state of the divalent cation to yield oxide or carbonate as the residual solid, together with gaseous products. The residual phases formed on decomposition of the transition metal malonates, including the nickel, cobalt and copper salts, depended on the atmosphere present and reactions involving the methylene group can result in cation reduction to yield metal and sometimes carbide [6,8–10].

The thermal reactions of some metal malonates, including those of calcium and of silver, were shown to proceed in the solid state [3,5]. In contrast, the thermal decomposition of the copper salt [4] proceeded with melting, during the first of two consecutive rate processes, when there was intermediate production of acetate and stepwise cation reduction ($Cu^{2+} \rightarrow Cu^{+} \rightarrow Cu^{0}$).

It has been demonstrated that acetate is formed as an intermediate during the decompositions of several malonates, examples include: the calcium [3], copper [4] and nickel [6,9,10] salts. This requires a hydrogen transfer step [3]. The principal objective of the present work was to investigate further the role of hydrogen transfer in these processes through comparative studies of the decompositions of cobalt malonate and of cobalt hydrogen malonate in atmospheres of nitrogen (inert), hydrogen and oxygen. The research was undertaken to determine whether hydrogen, present as a gas or in the acid salt, increased the overall decomposition rate of cobalt malonate. Greater availability of hydrogen might be expected to facilitate the formation of cobalt acetete, a probable interemediate, thereby promoting anion breakdown in cobalt malonate. A similar study of the comparable nickel salts has been published recently [9].

A previous study of the decomposition of cobalt malonate [8], under differential and accumulatory conditions, identified the products from vacuum reaction as mainly CO_2, with smaller amounts (17%) of CO, and the solid residue contained Co, CoO and Co_2O_3. In oxygen the reaction yielded CO_2 together with an oxide mixture including CoO, Co_2O_3 and Co_3O_4. The presence of water vapour at the interface accelerated the decomposition.

2. Experimental

2.1. Materials

The two cobalt malonate salts were prepared according to Levy et al. [11] as follows:

2.1.1. Cobalt malonate

0.050 mol $CoCl_2 \cdot 6H_2O$ (Koch Light, England) was added slowly, with stirring, to an aqueous solution of 0.050 mol disodium malonate (BDH, England) in 400 ml of distilled water (maintained at 60°C for 3 h). The precipitate was filtered, washed and finally dried at 100°C.

2.1.2. Cobalt hydrogen malonate

0.060 mol $CoCl_2 \cdot 6H_2O$ was added slowly, with stirring, to a solution of 0.120 mol malonic acid (Carlo Erba, Italy) in 200 ml of distilled water at ambient temperature. The precipitate was filtered, washed several times and finally dried at 100°C.

All chemicals used in these preparations were Analytical Grade materials and were used as received, without further purification.

2.2. Techniques

2.2.1. Elemental analysis

The carbon and hydrogen contents of each reactant used were determined by standard combustion analysis techniques. The amounts of cobalt in each salt were determined using the inductively coupled plasma method (ICP) with model OES ARL (Switzerland).

2.2.2. Thermal analysis

Thermal analyses measurements (thermogravimetry, TG, derivative thermogravimetry, DTG, differen-

tial thermal analysis, DTA, and differential scanning calorimetry, DSC) were carried out by means of a Shimadzu 'Stand Alone' thermal analyzer (TGA-50H, DTA-50 and DSC-50), Japan. The thermal analyzer is equipped with a data acquisition and handling system (TA-50WSI).

Thermal analysis experiments were performed in a dynamic atmosphere (flow = 40 ml/min) of N_2, H_2 or air at heating rates between 2 and 20°C/min. Experiments were normally carried out three times and each reported mass loss is an average of three measurements for data that agreed to better than 1%. Air, as a dynamic atmosphere, was excluded from the DSC experiments to avoid possible oxidation of the copper pans of the instrument. To remove the effects of variations of sample masses and particle sizes on the thermal analysis responses (e.g., peak shape and peak temperature) [12], equal masses (ca. 10–15 mg) of gently crushed samples of reactants were always used. The TG instrument was recalibrated at frequent intervals, accuracy was always better than ±0.1 mg.

Highly sintered α-Al_2O_3 powder (Shimadzu) was used as the reference material in DTA and DSC experiments. Calibration of both DTA and DSC instruments for temperature and enthalpy measurements were carried out using Specpure indium and zinc metals: melting points were 156.3 and 419.6°C, $\Delta H = 28.24$ and 101.50 J/g, respectively [13].

2.2.3. IR spectroscopy

IR spectra of both reactants, of samples partially decomposed at selected temperatures (under the different dynamic atmospheres) and of the solid products of each decomposition were carried out by the KBr disk technique using a Magna-FTIR 560 (USA) instrument operated by Nicolet Omnic software.

2.2.4. X-ray diffraction

X-ray powder diffraction analyses of the prepared reactants and their solid decomposition products were carried out using a Model D5000 Siemens diffractometer (Germany), Ni-filtered CuKα radiation ($\lambda = 1.5406$ Å). An on-line data acquisition and handling system permitted an automatic JCPDS library search and match (Diffrac AT software, Siemens) for phase identification.

2.2.5. Gas chromatography

The volatile decomposition products from both malonate reactants were analyzed by means of a Shimadzu computerized gas chromatograph Model GC-14A (Japan), connected with a flow system at atmospheric pressure. Gaseous products were sensed by a thermal conductivity detector. Automatic sampling was performed with a heated gas sampling valve, Type HGS-2.

2.3. Data processing

Kinetic parameters, i.e. the activation energy (E_a, kJ/mol) and the frequency factor (A/min), were calculated for both the dehydration and the decomposition processes observed from the DTG data using the Ozawa equation [14–16]

$$\ln\left(\frac{\beta}{T_m^2}\right) = \ln\left(\frac{AR}{E_a}\right) - \frac{E_a}{RT_m}$$

where β is the heating rate (K/min), T_m is the DTG peak maximum temperature, R is the gas constant.

DSC measurements were used to calculate the enthalpy change, ΔH for the dehydrations and the decompositions [17].

3. Results

3.1. Elemental analysis

The results of elemental analysis of both reactants, as prepared, are as follows (theoretical values, in brackets, were calculated for the dihydrate):

CoMal salt [$CoC_3H_2O_4 \cdot 2H_2O$]: 19.4% C (18.29); 3.3% H (3.07) and 30.23% Co (29.91).

CoHMal salt [$CoC_6H_6O_8 \cdot 2H_2O$]: 25.3% C (23.94); 4.3% H (3.35) and 19.83% Co (19.57).

The results for cobalt malonate are consistent with expectation for the dihydrate. These results also showed that cobalt hydrogen malonate salt is present as a dimer and the crystal contained two molecules of water.

3.2. Thermal analyses

3.2.1. Cobalt malonate dihydrate (CoMal)

Fig. 1 shows the TG, DTA and DSC curves for the decomposition of CoMal in a dynamic N_2 atmosphere

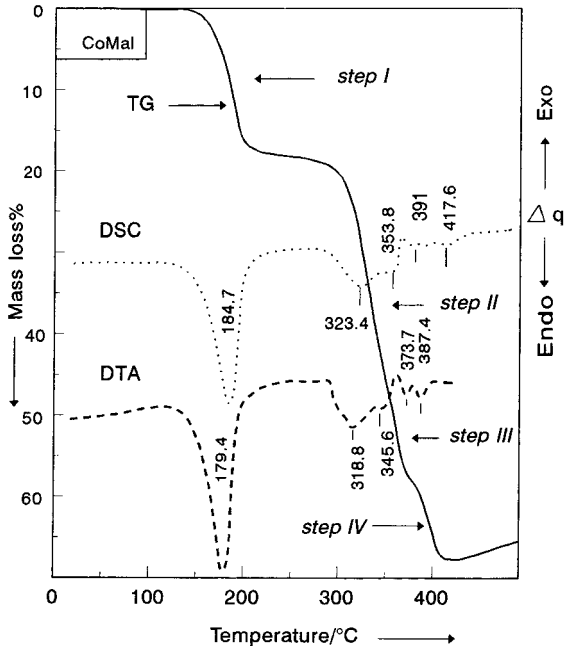

Fig. 1. TG, DTA and DSC curves for the decomposition of CoMal at a heating rate of 5°C/min under a dynamic atmosphere (40 ml/min) of N_2.

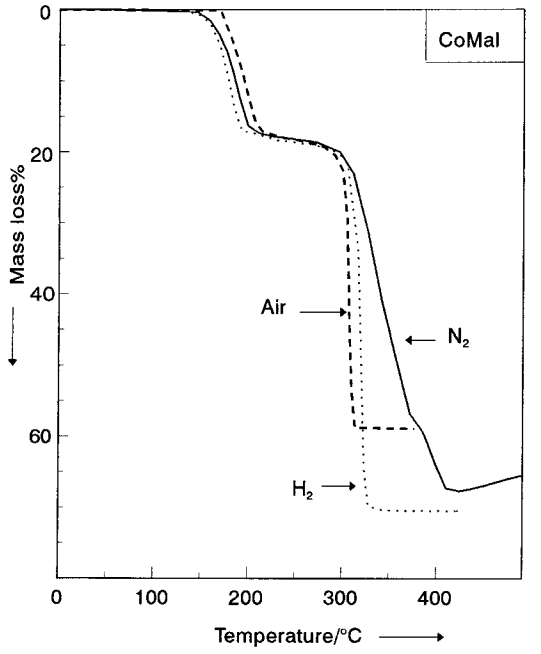

Fig. 2. Three TG curves for the decomposition of CoMal performed at a heating rate of 10°C/min in a dynamic atmosphere (40 ml/min) of N_2 (—), H_2 (···) and air (- - - -).

(40 ml/min). The TG curve shows four mass loss steps (labeled I–IV). The first step takes place between 140 and 220°C (18.05% mass loss) and is attributed to the dehydration of the reactant dihydrate to the anhydrous salt ($-2H_2O = 18.29\%$). This was followed by and overlapped with the second and third steps (280–366°C) which together result in 38.93% mass loss. The fourth, and last, step (370–415°C) is accompanied by 10.66% mass loss. This brings the total mass loss, after complete decomposition, to 67.64% of the original sample mass. Steps II–IV represent the decompositions of different reaction intermediates. Above 420°C, however, there was a small mass gain (which did not exceed 2%) which is attributed to the oxidation of a lower oxide (e.g., $CoO \rightarrow Co_2O_3$) due to traces of oxygen in the N_2 gas [18].

The DTG curve for CoMal decomposition showed four peaks of maximum rates of mass loss located at 188, 331, 364 and 394°C. The DTA curve for the decomposition of CoMal in N_2, Fig. 1, showed a broad endothermic peak at 179°C (due to the dehydration process). This was followed by four endothermic processes attributed to decomposition steps. The DSC curve (Fig. 1) exhibited the same characteristics as those of the DTA curve.

The effects of H_2 and of air atmospheres on the decomposition of CoMal are shown in Fig. 2 where the two TGA curves are compared with that in N_2 (all at the same rate of heating, 10°C/min). From this comparison, the following differences were found

1. Decomposition in H_2 or in air proceeded through only two mass loss steps, in contrast with four in N_2.
2. Decompositions were completed at appreciably lower temperatures in H_2 (at 320°C) and in air (310°C) compared with 420°C in N_2.
3. The total mass loss measured varied according to the composition of the prevailing dynamic atmosphere in the following sequence: in H_2 (70.15%) > in N_2 (67.64%) > in air (58.92%).

The mass loss in H_2 (70.15%) is very close to that expected for the formation of cobalt metal (70%), and this is probably also the predominant product from the decomposition in N_2. In air, however, the mass loss (58.92%) is close to that expected (59.26%) for the production of Co_3O_4.

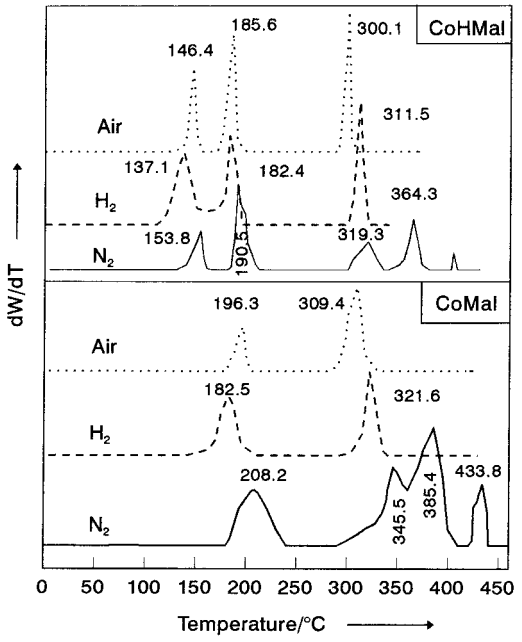

Fig. 3. DTG curves for the decomposition of CoMal and CoHMal at a heating rate of 10°C/min under different atmospheres of N_2 (—), H_2 (- - - -) and air (· · ·).

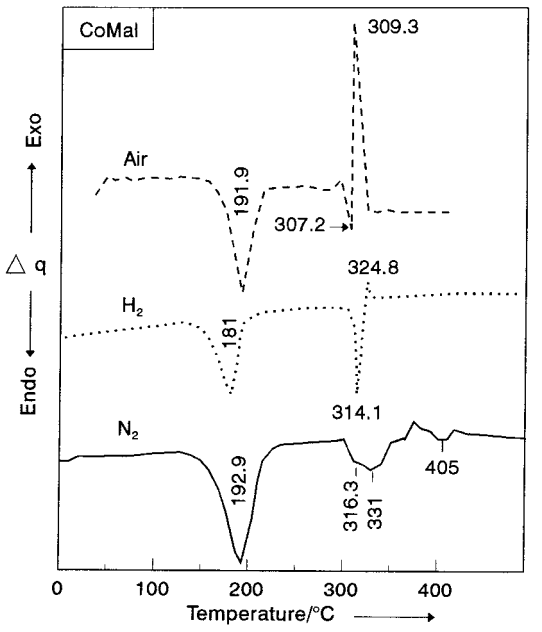

Fig. 4. Three DTA curves for the decomposition of CoMal carried out at a heating rate of 10°C/min in N_2 (—), H_2 (· · ·) and air (- - - -).

4. The mass gain process that was detected during the final stages of reactions in N_2 (above 420°C) disappeared completely in H_2 and in air.

The effects of variations of the prevailing atmosphere on the DTG curves for the decomposition of CoMal are shown in Fig. 3. Again, the presence of H_2 or air decreased the number of DTG responses to two peaks only, one for dehydration while the second is attributed to the completed decomposition, in contrast with the four peaks in N_2.

Fig. 4 shows, again, the effect of these reactive atmospheres (H_2 and air) on the decomposition of CoMal. The DTA curve in H_2 shows two endothermic peaks at 181°C (dehydration) and 314°C (decomposition). In air, however, the DTA curve shows an endothermic peak with the maximum at 192°C, attributed to the dehydration, while the decomposition appears as a sharp exothermic peak at 309°C.

3.2.2. Cobalt hydrogen malonate dihydrate (CoHMal)

Fig. 5 shows the TG, DTA and DSC curves for CoHMal decomposition in a N_2 atmosphere during

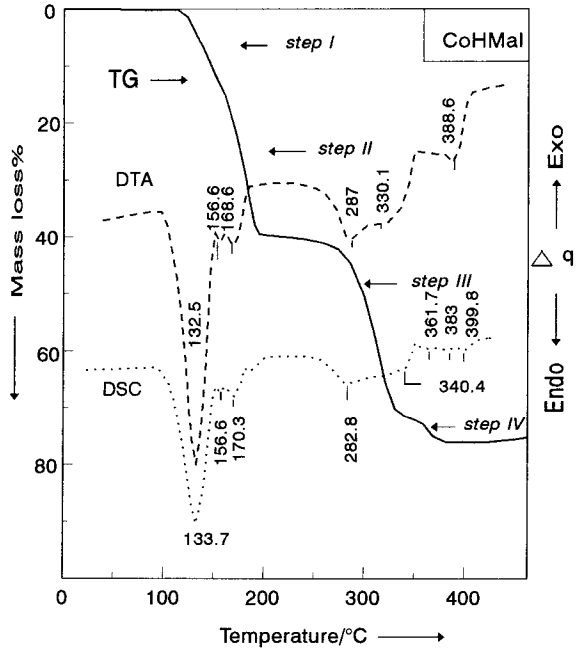

Fig. 5. TG, DTA and DSC curves for the decomposition of CoHMal at a heating rate of 5°C/min under a dynamic atmosphere (40 ml/min) of N_2.

heating at 5°C/min. The TG curve displays four mass loss steps (labeled I–IV) 112–160, 160–210, 250–350 and 350–390°C, respectively. These steps are associated with mass losses of 14.57, 25.63, 31.65 and 4.43%, respectively, representing a total mass loss of 76.28%. Above 420°C, there was a slight mass gain, after completion of decomposition, which did not exceed 1% of the original sample mass.

The first mass loss step is attributed to dehydration ($-2H_2O = 11.97\%$), together with a small amount of decomposition. This is followed by, and overlapped with, the second step which could be attributed to partial decomposition of the anhydrous salt to form a relatively stable (about 210–250°C) compound. The third and fourth steps represent two decomposition processes involving the formation of intermediates. The solid product undergoes some oxidation, above 420°C, (detected as a mass gain step) again ascribed to the presence of traces of oxygen in the N_2 gas. The corresponding DTG curve (Fig. 3) for decomposition of CoHMal in N_2 shows four peaks with maximum rates of mass losses at 154, 191, 319 and 364°C, respectively.

The DTA curve for CoHMal, Fig. 5, shows six endotherms. The first (at 132.5°C) is attributed to dehydration. This is followed by two small endotherms (at 157 and 169°C) ascribed to partial decomposition of the anhydrous salt. The first peak of these two endotherms disappeared at higher heating rates (>5°C/min). The remaining three endotherms are attributed to the different decomposition steps (at 287, 330 and 389°C).

The DSC curve, Fig. 5, is very similar to the DTA curve except for the splitting of the last decomposition step into three small peaks (at 362, 383 and 400°C).

The effects of H_2 or air atmospheres on the decomposition of CoHMal are shown in Fig. 6, which displays three TG curves (all at 10°C/min) for reactions in H_2, air and N_2 (for comparison). The following differences were found:

1. The detection of three mass loss steps only, the fourth step that was seen in N_2 has completely vanished.
2. The decompositions were completed at relatively lower temperatures in H_2 (320°C) and in air (310°C), compared with N_2 (390°C).

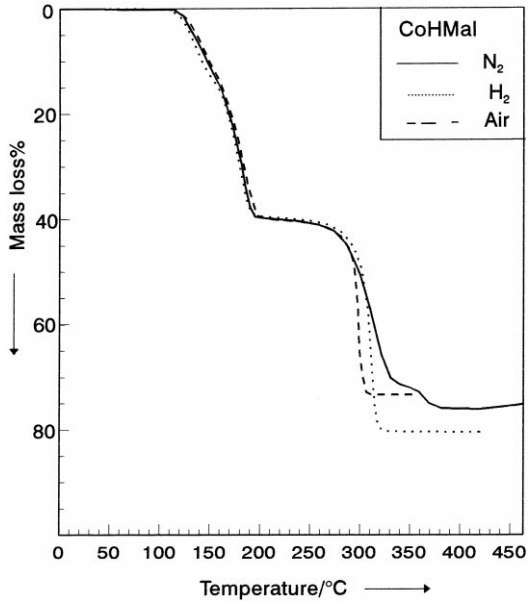

Fig. 6. Three TG curves for the decomposition of CoHMal performed at a heating rate of 10°C/min under a dynamic atmosphere (40 ml/min) of N_2 (—), H_2 (···) and air (- - - -).

3. The total mass losses calculated for the completed decompositions varied with the prevailing dynamic atmosphere used. These were 80.36% in H_2, 73.28% in air, compared with 76.28% in N_2. This, again, identifies cobalt metal as the major solid product from decomposition in H_2, CoO and cobalt metal are given in N_2, while Co_3O_4 predominates in air.

The effects of the prevailing atmosphere on the DTG curves for the decomposition of CoHMal are also shown in Fig. 3.

Fig. 7 shows the effect of H_2 or of air on the DTA curves of CoHMal (heated at 10°C/min) including for comparison a response curve for reaction in N_2. Two points of difference were recognized.

1. The several decomposition steps taking place in N_2 appear as one single process (a sharp endothermic peak in H_2 at 304°C or a sharp exothermic peak at 311°C in air).
2. Decompositions were completed at much lower temperatures (i.e., about 100°C lower than in the N_2 atmosphere).

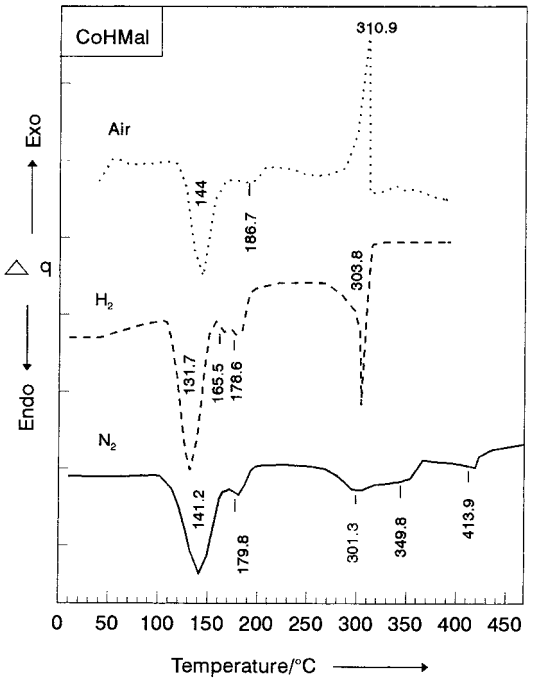

Fig. 7. Three DTA curves for the decomposition of CoHMal carried out at a heating rate of 10°C/min under a dynamic atmosphere of N_2 (—), H_2 (- - - -) and air (· · ·).

3.2.3. Kinetic and thermodynamic parameters

The kinetic parameters, activation energy (E_a/kJ/mol) and the frequency factor (A/min) together with the enthalpy changes (ΔH/kJ/mol) for the dehydrations and decompositions of both salts are given in Tables 1 and 2, respectively.

From Table 1, we draw attention to the following points

1. The activation energy (E_a) for the dehydration of CoMal (62 kJ/mol) is smaller than values reported previously (83.6 kJ/mol) [19]. The ΔH_{dehyd} (95 kJ/mol) value is smaller than those reported [20] by Ghosh et al. (113 kJ/mol) and by Galwey et al. [8], (107 kJ/mol).
2. E_a values for the decomposition steps in N_2 are consistent with the dimer structure of CoHMal. The magnitude of E_a for the first decomposition step of CoMal (146 kJ/mol) is significantly larger than that for CoHMal (94 kJ/mol). Also, E_a for the second decomposition step of CoHMal (233 kJ/mol) is about twice the value (116 kJ/mol) for CoMal.
3. The magnitudes of E_a for the dehydration and the first decomposition steps for reactions of both salts in a N_2 atmosphere were always less than those measured in H_2 or air, which is in accordance with results from a similar comparative study of some metal malonates [21].

3.2.4. IR spectroscopy

Figs. 8 and 9 show the IR transmission spectra for the hydrates of CoMal and of CoHMal, together with the spectra of samples decomposed at the selected

Table 1
Arrhenius parameters for the dehydrations and decompositions of cobalt malonate dihydrate and cobalt hydrogen malonate dihydrate in different atmospheres[a]

Arrhenius parameters	Step in the TG curve	CoMal			CoHMal		
		N_2	H_2	Air	N_2	H_2	Air
E_a (kJ/mol)	I (dehyd)	62 ± 3 (0.998)	94 ± 4 (0.989)	125 ± 6 (0.987)	65 ± 4 (0.992)	94 ± 4 (0.993)	101 ± 5 (0.959)
	II (decomp)	146 ± 7 (0.997)	234 ± 12 (0.979)	210 ± 10 (0.987)	94 ± 5 (0.991)	109 ± 6 (0.994)	165 ± 8 (0.955)
	III (decomp)	116 ± 6 (0.996)	– –	– –	233 ± 12 (0.997)	136 ± 6 (0.987)	260 ± 13 (0.986)
	IV (decomp)	71 ± 4 (0.986)	– –	– –	56 ± 3 (0.984)	– –	– –
ln (A/min)	I (dehyd)	14 ± 1	24 ± 2	32 ± 2	18 ± 1	27 ± 2	29 ± 2
	II (decomp)	29 ± 2	48 ± 3	43 ± 3	24 ± 2	38 ± 3	43 ± 3
	III (decomp)	20 ± 2	–	–	47 ± 3	28 ± 2	55 ± 3
	IV (decomp)	10 ± 1	–	–	10 ± 1	–	–

[a] Correlation coefficient for each plot [14–16] is shown in brackets under each E_a value.

Table 2
Enthalpy values (ΔH/kJ/mol) for the dehydrations and decompositions of CoMal and CoHMal in N_2 and H_2 atmospheres

Atmosphere	CoMal				CoHMal			
	Step 1	Step 2	Step 3	Step 4	Step 1	Step 2	Step 3	Step 4
N_2	95 ± 3	46 ± 2		11 ± 0.4		147 ± 4	69 ± 3	12 ± 0.7
H_2	48 ± 2	14 ± 0.7	–	–	–	59 ± 2	18 ± 1	–

temperatures and atmospheres specified. The following observations summarize the IR results

1. The differences between the spectra of the two parent salts are attributed to the variation in the crystal structures, see Fig. 8.
2. Above 200°C, the spectra of both salts became identical and showed evidence of the formation of cobalt acetate. This was concluded from the appearance of new peaks at 2933 and 2922/cm, which are attributed to the ν-CH_3 group [22], and at 1020 and 1050/cm, attributed to the acetate anion [23], see Fig. 9.
3. Between 250 and 300°C, two very sharp, strong peaks appeared at 1570 and 1418/cm which are attributed to surface carbonate species [24]. These two peaks were also seen when the decompositions of both salts were performed in H_2 or in air, see Fig. 9.
4. At higher temperatures (about 350°C), peaks due to surface carbonate species have vanished and the only peaks remaining are those between 650–250/cm, attributed to metal oxygen bonds [24], see Fig. 8. Two different oxides were formed, one in the presence of N_2 and H_2 with absorption peaks at 650 and between 560 and 340/cm attributed to CoO oxide [25]. In air, however, Co_3O_4 predominates with its absorption peaks at 665, 460 and 350/cm [26], see Fig. 9.

3.2.5. X-ray analysis

Fig. 10 shows the X-ray diffraction patterns (a–e) of the two parent salts CoMal (a) and CoHMal (b)

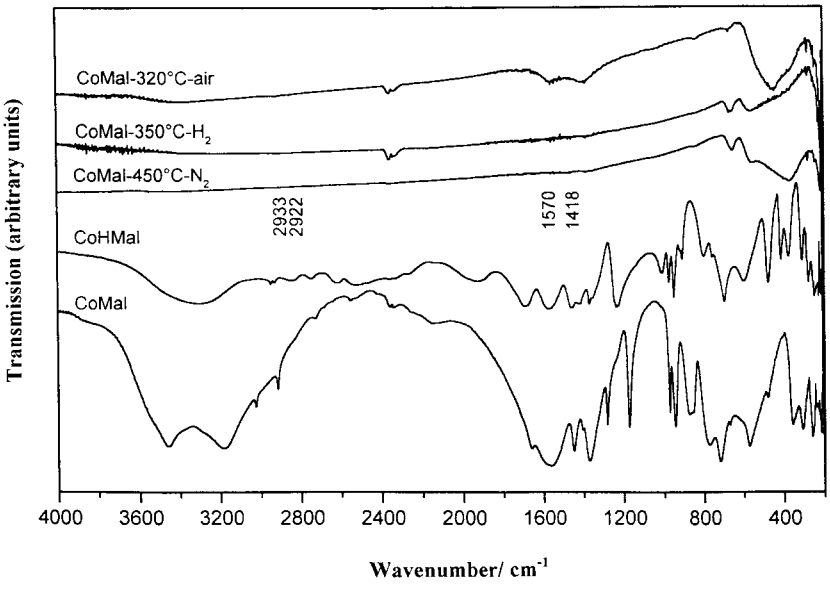

Fig. 8. IR transmission spectra for the original prepared dihydrates CoMal and CoHMal together with spectra of the final solid products after reaction in different atmospheres at the indicated temperatures.

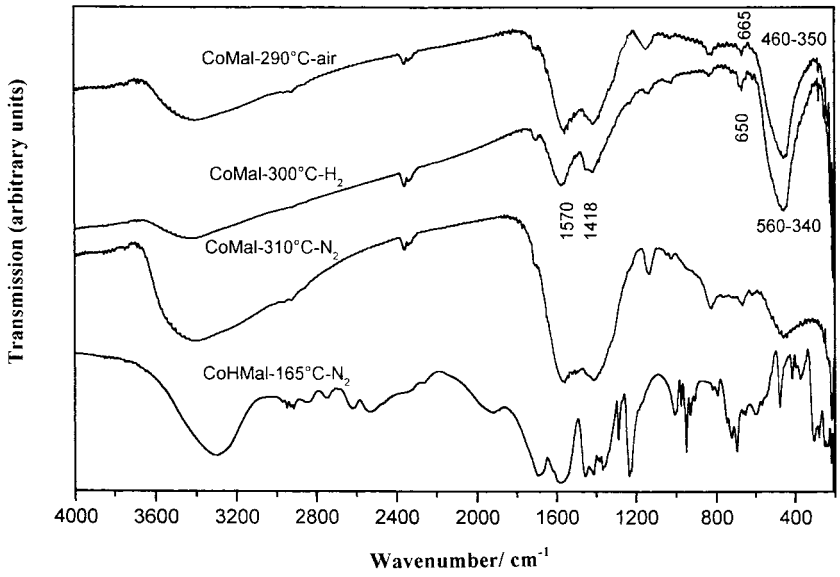

Fig. 9. IR transmission spectra for CoMal and CoHMal reactants after decomposition at some selected temperatures under different atmospheres.

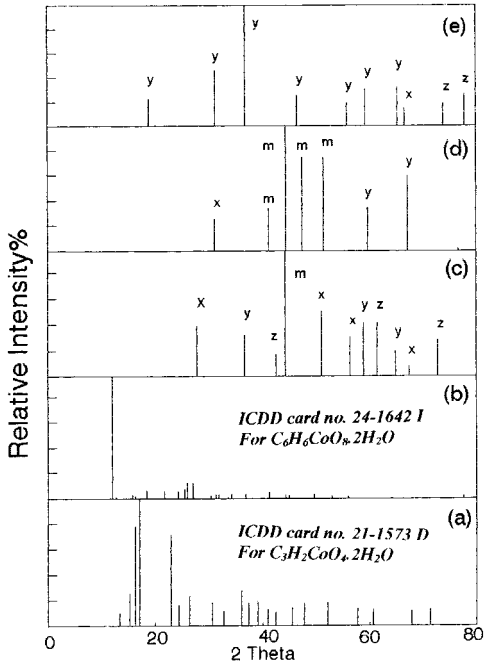

Fig. 10. XRD patterns for the original prepared dihydrates CoMal (a) and CoHMal (b) together with the final solid products after reaction in different atmospheres of N_2 at 450°C (c), H_2 at 360°C (d) and air at 350°C (e) (m: cobalt metal; x: Co_2O_3; y: Co_3O_4 and z: CoO).

together with the final solid decomposition products of CoMal and CoHMal after reaction in different atmospheres, i.e. at 450°C in N_2 (c), at 360°C in H_2 (d) and 350°C in air (e).

Diffraction patterns (a) and (b) for the two parent salts were found to match well with the standard ICDD Data [27]: No. 21-1573 D of the salt having the formula $C_3H_2CoO_4{\cdot}2H_2O$ of cobalt malonate dihydrate and 24-1642 I for the salt having the formula $C_6H_6CoO_8{\cdot}2H_2O$ of cobalt hydrogen malonate dihydrate. This confirms the identities of the reactants.

Pattern (c), for the decomposition products after reaction at 450°C in N_2, reveals that cobalt metal (ICDD Card No. 15-0806) is the major product. In addition, there are detectable amounts of CoO (ICDD Card No. 42-1300) and of Co_3O_4 (ICDD Card No. 42-1467). Similarly, pattern (d) for the decomposition product in H_2 (at 350°C) shows the predominant formation of cobalt metal.

The pattern for the solid decomposition product of CoMal in air (e), however, shows Co_3O_4 to predominate, together with smaller amounts of CoO and Co_2O_3.

X-ray diffraction results confirm the thermogravimetric (TG) conclusions, for both CoMal and CoHMal

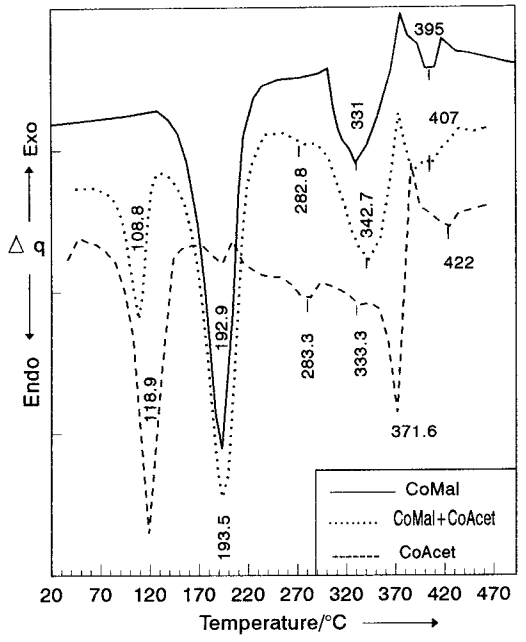

Fig. 11. Three DTA curves carried out at a heating rate of 10°C/min under a dynamic atmosphere (40 ml/min) of N_2 for pure CoMal (—), cobalt acetate tetrahydrate (- - - -) and a mixture of CoMal + 10% (by mass) of cobalt acetate (· · ·).

(see above), that cobalt metal predominates as the solid product in the presence of H_2 or N_2 atmospheres while Co_3O_4 and Co_2O_3 were the dominant phases from reaction in air. X-ray diffraction patterns from samples (of both salts), partially decomposed to different extents, gave evidence of the formation of some intermediate compounds. The most important of these was identified as cobalt acetate (ICDD Card No. 25-0372 D), cobalt oxalate (ICDD Card No. 14-0741 D) and cobalt oxide hydroxide, CoOOH (ICDD Card No. 26-0480 I).

To support further the identification of the intermediate formation of cobalt acetate, Fig. 11 shows three DTA experiments for CoMal, cobalt acetate tetrahydrate and a mixture of CoMal + 10% (by mass) of CoAcet heated at 10°C/min in N_2. From the similarity of the thermal behaviour, positions and sizes of peaks, between the DTA curves for pure CoMal and the CoMal + CoAcet mixture, we conclude that CoAcet is formed as an intermediate during the decompositions of CoMal. Similar experiments gave similar results for CoHMal.

3.3. Gas chromatography

The gaseous decomposition products from both salts (CoMal and CoHMal), after dehydration, were found to be similar. The most abundant volatile products detected were CO_2, CO, acetic acid and acetone. Traces of esters were also detected.

The presence of acetone among the volatile decomposition products and the formation of surface carbonate species (indicated by the IR results) confirms the formation of cobalt acetate as a reaction intermediate. Decomposition may thus include the following reactions:

$$(CH_3COO)_2\,Co \rightarrow (CH_3)_2CO + CoCO_3$$

4. Discussion

4.1. Dehydration

For both reactants, the mass loss during the first endothermic reaction was consistent with complete dehydration during a single rate process: cobalt malonate dihydrate-18.05%, DSC and DTA peak maxima at 182 ± 3°C and cobalt hydrogen malonate dihydrate- 14.57% (but overlapped with the onset of decomposition), DSC and DTA maxima at 133 ± 1°C. The variations in dehydration rates with change of atmosphere (N_2, H_2 or air) were relatively small (Figs. 2 and 6). The same reaction proceeded in comparable temperature intervals and it is improbable that these gases participate in the water elimination steps. The kinetic parameters for dehydration of carboxylates, e.g., nickel oxalate dihydrate [28], can be particularly sensitive to the prevailing reaction conditions, most notably the availability of water vapour in the vicinity of the reactant. Rates of many endothermic, reversible rate processes are influenced to significant extents by self-cooling and equilibria displacements, together with parameters other than the rate controls of the surface or interface dissociation step. This sensitivity of kinetic characteristics to conditions explains the variations of apparent values of E_a (62–125 kJ/mol, Table 1) and the activation energy cannot be associated with an identified rate limiting step.

4.2. Cobalt malonate decomposition

The kinetics of cobalt malonate decomposition are sensitive to the atmosphere present, Figs. 1–4. The temperatures of reaction in air (about 280–320°C) or in H_2 (about 305–340°C), from Fig. 3, were similar. These are comparable with those for nickel malonate decomposition (see Fig. 3 of [9]). The decomposition of cobalt malonate in N_2, however, occurred in a slightly higher temperature range (350–390°C).

4.2.1. Reaction in hydrogen

The principal residual product was identified as cobalt metal. The oxide is also present, detected by X-ray diffraction, and could arise from atmospheric oxidation following solid product removal from the reaction vessel; many metals are formed in a finely divided state during carboxylate breakdown and some are even pyrophoric [29,30]. The calculated value of E_a for this reaction (234 kJ/mol) is somewhat larger than for decomposition in air or in N_2 and also for the reaction under accumulatory conditions (180 kJ/mol [8]).

4.2.2. Reaction in air

This reaction resulted in the formation of residual oxide, principally Co_3O_4, the reaction temperature was just detectably lower than that for decomposition in H_2. Previous comparative studies [31] showed that the accumulatory decomposition of nickel malonate (and some related salts) and its reaction in oxygen occurred at comparable temperatures (and also maintained similar kinetic characteristics). However, when oxygen was present in sufficient amounts, the carbon in each of the several anions studied [31] was comprehensively oxidized to carbon dioxide. The closely similar reactivities and behaviour, during reactions of cobalt malonate in H_2 and in air, may be ascribed to the heterogeneous promotion of anion breakdown by an interface process occurring on the surface of the solid product, as for the decompositions of many solid state reactants [1,2,8]. The reactivity-controlling parameter is identified as an electron transfer step [32,33] at the residual, cobalt metal or cobalt oxide (CoO is a p-type semiconductor) accompanied, or closely followed, by breakdown of the anion, destabilized by loss of the bond with the cation. (Malonic acid decomposes below 150°C, to acetic acid and carbon dioxide). Surface-bonded products of malonate degradation will either undergo further heterogeneous reactions with dissociated hydrogen or, in oxygen, be oxidized to CO_2: by either path, the carbonaceous products from the reacted material are rapidly volatilized from the active reaction zone. The catalytically active surface is thereby regenerated to remain available as an electron-donating source for proximate anions and reaction continues. The stability and reactivity of the reactant anionic species are, therefore, identified as the controlling parameters in the decomposition, under conditions of active regeneration of the promoting surface. This also accounts for the close similarity of decomposition rates of both cobalt and nickel salts, in H_2 and in air.

The reaction in N_2 differs in that the overall ability of the solid reaction products to promote the anion breakdown, composed of the metal and all three cobalt oxides detected, is significantly less than in the presence of either H_2 or O_2. This can be ascribed to the formation of surface-adsorbed species that persist in the absence of reaction in the presence of a 'surface-cleaning' reactive-gas adsorbent (i.e., H_2 or O_2). The delayed or inhibited surface breakdown of adsorbed malonate, and other anionic species, which probably include acetate, carbonate and oxalate (IR data and Fig. 11), accounts for the several distinct responses (reactions) at temperatures above those at which the reactions proceed in H_2 or in air. These contributory reactions are further modified by the presence of trace amounts of O_2 (in the N_2 gas). This is probably sufficient to deactivate the surface, by competing with malonate anions for the active sites, but the quantities present are insufficient to remove rapidly the accumulated organic residues resulting from the anion breakdown steps. Taken with the other observations (Figs. 8, 9 and 11), this model is entirely consistent with the view that acetate is formed as an intermediate in the thermal decomposition of cobalt malonate.

4.3. Cobalt hydrogen malonate decomposition

The most obvious differences between the thermal reactions of cobalt hydrogen malonate and of cobalt malonate were the temperatures of dehydration and, for the hydrogen salt, an endothermic decomposition at about 182–191°C (Fig. 3). The difference in dehydration temperatures is not unexpected for different

substances having different crystal structures (Fig. 10) and has been referred to above.

The subsequent higher temperature reactions of the hydrogen salt (above 250°C) show a very close similarity of behaviour and pattern of variations in the different atmospheres with those observed for cobalt malonate (compare Fig. 1 with 5, 2 with 6, 4 with 7 and 3). The most obvious and reasonable explanation is that cobalt malonate is the product of breakdown of cobalt hydrogen malonate that occurred during the endothermic reaction at about 180°C. This is the same pattern of reactions as those reported previously for the nickel salts [9]. There are relatively minor differences in peak maxima between the two cobalt salts attributable to variations in particle sizes for the reactants, both of which have been dehydrated but only one of which has undergone the low temperature decomposition.

The endotherm at 182–191°C during heating of cobalt hydrogen malonate must, therefore, be identified with the loss of malonic acid, which may be represented:

$$(HOOC{-}CH_2{-}COO)_2Co \rightarrow CH_2(COO)_2Co + CH_2(COOH)_2$$

This is undoubtedly a simplification because the production of malonic acid is expected to be accompanied by some rapid decomposition, at these reaction temperatures, to CO_2 and acetic acid (acetic anhydride and/or ketene and water [5]). As expected, this rate process is effectively independent of the gaseous atmosphere present and the rapid removal of all volatile products in the gas stream is consistent with the identity of the subsequent reactions with those for the decomposition of cobalt malonate.

4.4. Comment

It is concluded that the decomposition of cobalt malonate occurs at a reactant-product interface [8] in common with very many solid state crystolysis reactions [1,2,5]. Because the absolute rates of this reaction in H_2 and in air (oxygen) are closely similar, we conclude that, despite the different product phases, both reactions are controlled by an electron transfer step from the solid product (metal or oxide, respectively), after which the anion breaks down. During reactions in these gases, no carbonaceous residues accumulate on the active surfaces due to secondary chemical changes. In nitrogen, however, the catalytic function of the solid surface becomes inhibited through the accumulation of organic residues and oxide/adsorbed oxygen, because insufficient reactive adsorbed gas is available to remove them, by reduction or by oxidation.

This is evidence of the possibility that gases present may participate in the interface reactions during crystolysis, a topic [1,2,31] that has probably received less attention than its importance warrants. The present work also emphasizes the similarities that may be found between the kinetics of thermal decompositions of solids and heterogeneous catalytic reactions, transition metals are active in promoting the breakdown of carboxylic acids.

We are reluctant to propose mechanistic reaction models or to identify a rate limiting step on the basis of the kinetic observations for the dehydration reactions. This is a consequence of the sensitivity of the rates of these reactions to prevailing conditions [28], most notably the availability of water within the reaction zone.

Those reactions occurring after the endothermic first step in the decomposition of cobalt hydrogen malonate were as expected for the breakdown of cobalt malonate. It is, therefore, concluded that the volatile products from this first reaction of the anion exert no significant influence on the course of the subsequent decompositions.

A principal objective of this work was to determine whether the hydrogen present as a gas or in the acid salt increased the production of cobalt acetate as a reaction intermediate. The present observations supported the view that, as with other transition metal malonates, there was the intermediate formation of acetate during cobalt malonate decomposition. However, there was no evidence that these forms of available hydrogen, present as a gas or in the acid salt, enhanced the production of cobalt acetate or appreciably changed the kinetics or mechanism of the decomposition of cobalt malonate.

References

[1] M.E. Brown, D. Dollimore, A.K. Galwey, in: C.H. Bamford, C.F. Tipper (Eds.), Reactions in the Solid State (Comprehensive Chemical Kinetics, vol. 22), Elsevier, Amsterdam, 1980

[2] A.K. Galwey, M.E. Brown, Thermal Decomposition of Ionic Solids, Elsevier, Amsterdam, 1999.
[3] A.K. Galwey, M.A. Mohamed, Solid State Ionics 42 (1990) 135.
[4] N.J. Carr, A.K. Galwey, Proc. R. Soc., London A 404 (1986) 101.
[5] A.K. Galwey, M.A. Mohamed, J. Chem. Soc. Faraday Trans. I 81 (1985) 2503.
[6] A.K. Galwey, S.G. McKee, T.R.B. Mitchell, M.A. Mohamed, M.E. Brown, A.F. Bean, React. Solids 6 (1988) 187.
[7] K. Muraishi, Y. Suzuki, Y. Takahashi, Thermochim. Acta 286 (1996) 187.
[8] A.K. Galwey, D.M. Jamieson, M. Le Van, C. Berro, Thermochim. Acta 10 (1974) 161.
[9] M.A. Mohamed, A.K. Galwey, S.A. Halawy, Thermochim. Acta 323 (1998) 27.
[10] M.A. Mohamed, J. Anal. Appl. Pyrolysis 30 (1994) 59.
[11] L.W. Levy, J. Perrotey, J.W. Visser, Bull. Soc. Chim. France 9-10 (1973) 2596.
[12] M.A. Mohamed, S.A. Halawy, J. Thermal Anal. 41 (1994) 147.
[13] R.C. Weast (Ed.) Handbook of Chemistry and Physics, 62nd edn., CRC Press, New York, 1982.
[14] T. Ozawa, J. Bull. Chem. Soc. Japan 38 (1965) 1881.
[15] T. Ozawa, Thermal. Anal. 2 (1970) 301.
[16] T. Ozawa, Thermal. Anal. 7 (1975) 601.
[17] A. Mohamed, S.A.A. Mansour, M.I. Zaki, Thermochim. Acta 138 (1989) 309.
[18] K. Muraishi, K. Nagase, N. Tanaka, Thermochim. Acta 23 (1978) 125.
[19] N. Nagase, K. Muraishi, K. Sone, N. Tanaka, Bull. Chem. Soc. Japan 48 (1975) 3184.
[20] S. Ghosh, S.K. Ray, P.K. Ray, T.K. Banerjee, J. Ind. Chem. Soc. LXI (1984) 850.
[21] S. Shishido, K. Ogasawara, Sci. Rep. Niigata Univ. Ser. C 3 (1971) 23.
[22] J.R. Ferraro, Low Frequency Vibration of Inorganic and Coordination Compounds, Plenum Press, New York, 1971
[23] P. Baraldi, Spectrochim. Acta, Part A 38 (1982) 51.
[24] K. Nakamoto, Infrared Spectra of Inorganic and Coordination Compounds, Wiley, London, 1963.
[25] R.A. Nyquist, R.O. Kogal, Infrared Spectra of Inorganic Compounds, Academic Press, New York, 1971, p. 219.
[26] N.T. McDevitt, W.L. Baun, Spectrochim. Acta 20 (1964) 799.
[27] JCPDS-ICDD, PDF2 Data Base 1996.
[28] T.B. Flanagan, J.W. Simons, P.M. Fichte, Chem. Commun. (1971) 370.
[29] A.K. Galwey, P. Gray, J. Chem. Soc. Faraday Trans. I 68 (1972) 1935.
[30] A.K. Galwey, P. Gray, J. Chem. Soc. Faraday Trans. I 70 (1974) 1018.
[31] B.R. Wheeler, A.K. Galwey, J. Chem. Soc. Faraday Trans. I 70 (1974) 661.
[32] R.J. Acheson, A.K. Galwey, J. Chem. Soc. A (1967) 1167
[33] M.A. Mohamed, A.K. Galwey, Thermochim. Acta 213 (1993) 269.